Reactions of Beryllium Atoms with Hydrogen. Matrix Infrared Spectra of Novel Product Molecules

Thomas J. Tague, Jr., and Lester Andrews*

Contribution from the Department of Chemistry, University of Virginia, Charlottesville, Virginia 22901

Received June 28, 1993®

Abstract: Beryllium atoms formed by pulsed laser ablation have been codeposited with gaseous mixtures of hydrogen diluted in argon (concentrations varied from 25:1 to 100:1) onto a substrate at 10 K. Infrared spectroscopy on the reaction mixture identified six novel product molecules—BeH, BeH_2, BeBeH, HBeBeH, HBeHBeH, and $HBe(H)_2$-BeH. Assignments of infrared absorption bands were made on the basis of broad-band photolysis and annealing behavior, isotopic substitutions, and ab initio calculations performed at the MBPT(2) level. The major products initially are BeH (1970.0 cm^{-1}) and the previously unobserved BeH_2 molecule ($v_3 = 2159.1$ cm^{-1}, $v_2 = 697.9$ cm^{-1}) with formation of the three dimers HBeBeH, HBeHBeH, and $HBe(H)_2BeH$ at the expense of the initial reaction products upon annealing of the matrix to 30 K. The former dimer involves a stable Be–Be bond, and the latter dimers incorporate bridging hydrogen atoms. The new Be_2H molecule (2013.7, 540.0 cm^{-1}) is a minor product in these experiments, which exhibits a stronger Be–Be bond than Be_2.

Introduction

Over the last 10–20 years the study of beryllium hydrides has been of considerable interest. Experimentally, these compounds are difficult to obtain pure, but solid BeH_2 is believed to have a hydrogen-bridging polymeric structure.[1–3] However, only BeH has been observed in molecular form in the gas phase by electronic spectroscopy,[4] and in solid argon by electron spin resonance spectroscopy,[5] and polymeric beryllium hydride in solution has been characterized by infrared spectroscopy.[6] Because beryllium is small and possesses high ionization and sublimation energies, lattice energies are insufficient to provide charge separation to form the Be^{2+} cation. Beryllium compounds therefore tend to be somewhat covalent in nature; even BeO and BeF_2 show substantial covalent character. While initially beryllium can form divalent molecules it has a tendency to achieve maximum coordination whenever possible.[7,8]

Owing to the small number of valence electrons, beryllium hydrides have been examined in numerous theoretical studies.[8–17] In particular, electronic structure calculations have predicted that BeH_2 is a linear molecule[3,17,18], and many introductory chemistry textbooks explain the bonding in linear BeH_2 using sp hybridization. Further geometry optimization studies have also

shown that HBeBeH is the favored dimer of BeH,[3,9,14,15] but the stable dimer of BeH_2 is the $HBe(H)_2BeH$ bridged compound.[3,9,15] Although Be_2 is a weakly bound molecule,[18] the addition of electron-withdrawing substituents substantially strengthens the Be–Be bond[14,16] and suggests that Be_2H and HBeBeH should be observable.

The matrix isolation technique is ideally suited for studying reactions of this type since the inert gas matrix prevents initial products from undergoing further reactions until they can be characterized spectroscopically. Additional reaction products can then be formed in a controlled manner by photolysis and matrix annealings.

Recent matrix infrared studies on boron, aluminum, and uranium atom reactions with O_2, CO, CO_2, and N_2 have demonstrated that Nd:YAG laser ablation is a clean and effective source of atomic vapor species.[19–26] The hyperthermal nature of pulsed laser evaporated atoms was necessary for many of these reactions to proceed. The primary purpose of this matrix study on beryllium atom reactions with hydrogen was to provide characterization of initial beryllium hydrides and then examine dimerization products. Reactions of beryllium atoms with O_2, N_2, CO, and CO_2 are also under investigation.[27–29]

Experimental Section

A beryllium metal (Johnson Matthey, lump, 99.5%) target was laser evaporated using a Quanta Ray DCR-11 Nd:YAG laser at 1064 nm in the Q switched mode with a 10-ns pulse duration. The laser power was typically 70 mJ/pulse at the sample with a 10-Hz repetition rate. Beryllium atoms formed as a result of this evaporation were codeposited with argon and H_2 (typical dilutions between 25:1 and 100:1) onto a cold

® Abstract published in *Advance ACS Abstracts*, November 1, 1993.

(1) Cotton, F. A.; Wilkinson, G. *Advanced Inorganic Chemistry*; Wiley-Interscience: New York, 1988.

(2) Head, E. L.; Holley, C. E.; Rabideau, S. W. *J. Am. Chem. Soc.* **1957**, *79*, 3687.

(3) Dill, J.; Schleyer, P. v. R.; Binkley, J. S.; Pople, J. A. *J. Am. Chem. Soc.* **1977**, *99*, 6159 and references therein.

(4) Huber, K. P.; Herzberg, G. *Molecular Spectra and Molecular Structure; Vol. 4: Constants of Diatomic Molecules*; Van Nostrand Reinhold Co.: New York, 1979.

(5) Knight, L. B., Jr.; Brom, J. M., Jr.; Weltner, W., Jr. *J. Chem. Phys.* **1972**, *56*, 1152.

(6) Bell, N. A.; Coates, G. E. *J. Chem. Soc.* **1965**, *74*, 692.

(7) Noth, H.; Schlosser, D. *Inorg. Chem.* **1983**, *22*, 2700.

(8) Canadell, E.; Eisenstein, O. *Inorg. Chem.* **1983**, *22*, 3856.

(9) DeFrees, D. J.; Raghavachari, K.; Schlegel, H. B.; Pople, J. A.; Schleyer, P. v. R. *J. Phys. Chem.* **1987**, *91*, 1857.

(10) Meyer, W.; Rosmus, P. *J. Chem. Phys.* **1975**, *63*, 2356 and references therein.

(11) Henriet, C.; Verhagen, G. *Phys. Scr.* **1986**, *33*, 299.

(12) Clerbaux, C.; Colin, R. *Mol. Phys.* **1991**, *72*, 471.

(13) Sana, M.; Leroy, G. *Theor. Chem. Acta* **1990**, *77*, 383.

(14) Jaisen, P. G.; Dykstra, C. E. *J. Am. Chem. Soc.* **1985**, *107*, 1891.

(15) Ahlrichs, R. *Theor. Chim. Acta* **1970**, *17*, 348.

(16) Bruna, P. J.; Di Labio, G. A.; Wright, J. S. *J. Phys. Chem.* **1992**, *96*, 6269.

(17) Sana, M.; Leroy, G.; Wilante, C. *Organometallics* **1991**, *10*, 264.

(18) Bondybey, V. E. *Chem. Phys. Lett.* **1984**, *109*, 436. Bondybey, V. E. *Science* **1985**, *227*, 125.

(19) Burkholder, T. R.; Andrews, L. *J. Chem. Phys.* **1991**, *95*, 8697.

(20) Hassanzadeh, P.; Andrews, L. *J. Phys. Chem.* **1992**, *96*, 9177.

(21) Burkholder, T. R.; Andrews, L. *J. Phys. Chem.* **1992**, *96*, 10195.

(22) Burkholder, T. R.; Andrews, L.; Bartlett, R. J. *J. Phys. Chem.* **1993**, *97*, 3500.

(23) Andrews, L.; Burkholder, T. R.; Yustein, J. T. *J. Phys. Chem.* **1992**, *96*, 10182.

(24) Hunt, R. D.; Andrews, L. *J. Chem. Phys.* **1993**, *98*, 3690.

(25) Hunt, R. D.; Yustein, J. T.; Andrews, L. *J. Chem. Phys.* **1993**, *95*, 9177.

(26) Tague, T. J., Jr.; Andrews, L.; Hunt, R. D. *J. Phys. Chem.* **1993**, *97*, 10920.

(27) Thompson, C. A.; Andrews, L., unpublished results.

(28) Thompson, C. A.; Andrews, L., unpublished results.

(29) Tague, T. J., Jr.; Andrews, L., unpublished results.

Table I. Infrared Absorption Band Positions (cm^{-1}), Photolysis and Annealing Behavior, and Product Molecule Identifications in the Be + H$_2$ System

H$_2$	D$_2$	photolysis/annealing[a]	product molecule
558		0/+50	HBe(H)$_2$BeH
540.0		0/−50	BeBeH
697.9	531.9	+30/−60	BeH$_2$
872	651	0/+50	HBe(H)$_2$BeH
1370	1053	0/×5	BeH$_2$ aggregate
1402.1		0/+50	HBeHBeH
1420	1067	0/+50	HBe(H)$_2$BeH
1493.4	1088	0/+50	HBeHBeH
1536	1094	0/+50	HBe(H)$_2$BeH
1900.6	1533.0	−60/×10	HBeBeH
1970.0	1477.6	+20/−60	BeH
1982	1567	0/+50	HBeHBeH
			HBe(H)$_2$BeH
2013.7	1504.2	0/−50	BeBeH
2159.1	1674.0	+30/−60	BeH$_2$

[a] Photolysis and annealing changes are indicated as percent changes except for annealing of HBeBeH which grows in by more than 10 times on annealing.

Table II. Energies and Frequencies Calculated for the Be + H$_2$ System at the MBPT(2) Level Using the 6-311G* Basis Set

molecule	energy (hartrees)	frequencies (cm^{-1})[a]
H	−0.49981	
Be	−14.61405	
BeH		2086.3
BeD	−15.18750	1548.2
BeH$_2$	−15.82396	2228.6, (2025.2), 747.3
BeD$_2$		1714.2, (1432.8), 574.8
BeHD		2150.4, 1551.0, 666.7
BeBeH	−29.84998	2114.9, 541.7
BeBeD		1574.6, 528.1
HBeBeH	−30.48462	(2131.5), 2104.2, (644.8), (604.6), 431.3
DBeBeD		(1604.0), 1561.5, (606.2), (500.1), 320.0
HBeBeD		2118.3, 1582.5, (625.5), 566.9, 361.4
HBeHBeH	−31.05326	2158.3, 1524.0, 1504.8
DBeDBeD		1608.8, 1116.3, 1089.8
HBe(H)$_2$BeH	−31.69849	2157.9, 1600.2, 1494.7, 948.0, 591.9
DBe(D)$_2$BeD		1612.9, 1198.0, 1088.2, 720.1, 430.2

[a] Infrared inactive bands are shown in parentheses.

substrate at 10 K. Under similar pulsed laser ablation conditions with beryllium metal, Bondybey observed primarily atomic Be with smaller amounts of Be$^+$ based on gas-phase emission spectra.[18] The substrate was a CsI optical window mounted in a copper retainer at the cold tip of a CTI Cryogenics Model 22 closed-cycle refrigerator suspended in a custom built vacuum chamber described earlier.[19,20] The laser beam was focused by a lens (focal length of 10 cm) through a hole in the CsI window onto the metal target. The metal target was rotated at 1 rpm to prevent boring and minimize metal cluster formation; laser tracks were 0.1 mm wide. The cold head of the refrigerator could be rotated under vacuum so that the substrate faced the target and gas deposition port or CsI windows for obtaining transmission FTIR spectra (Nicolet Model 750 and 5DXB FTIR spectrometers). The reported spectra are averages of 500 scans with spectral resolution of 0.5 cm^{-1} and band position accuracy of ±0.1 cm^{-1}. A 175-W medium-pressure mercury arc lamp (Philips H39KB) with the globe removed was used to photolyze the matrix at 1-h intervals through a quartz window. To further promote dimer formation, the argon matrix was annealed to between 15 and 30 K. IR spectra were recorded before and after sample deposition and after each photolysis/annealing. Since during photolysis annealing must also be occurring, the sequence of photolysis and annealing was interchanged in an effort to correlate product bands.

Extensive ab initio theoretical investigations for several possible product molecules found in this investigation have been previously conducted.[8-17] However, isotopic data are an integral part of this work, and since the literature is void of isotopic frequency calculations, ab initio calculations were performed at the MBPT(2) level using the ACES II program system and the 6-311G* basis set.[30] Agreement with the literature in calculated frequencies and geometries was complete for all molecules (±0.01 experiment/theory factor for frequencies and ±0.01 Å for interatomic distances). For uniformity in making band assignments, the MBPT(2) results calculated in our laboratory will be reported.

Results

Infrared spectra for the reaction of pulsed laser evaporated beryllium atoms with hydrogen will be presented. Six sets of product bands were observed and grouped by annealing and photolysis behavior, isotopic shifts, and ab initio calculations and are collected in Tables I and II.

Be + H$_2$. The diagnostic beryllium–hydrogen stretching region, 2200–1800 cm^{-1}, is shown in the top spectrum of Figure 1 after 3 h of codeposition of Be atoms with a 25:1 Ar/H$_2$ mixture. New product bands are found at 2159.1, 2013.7 (with a shoulder at 2001.5), 1982, 1970.0, and 1900.6 cm^{-1} (labeled 2, 3, 5 and 6, 1, and 4, respectively), which are tabulated in Table I. The photolysis and annealing behavior of these bands is shown in

(30) Stanton, J. F.; Gauss, J.; Watts, J. D.; Lauderdale, W. J.; Bartlett, R. J. ACES II, an Ab Initio System for Coupled Cluster and Many-Body Perturbation Theory Methods. *Quantum Theory Project*; University of Florida: Gainsville, FL, 1992.
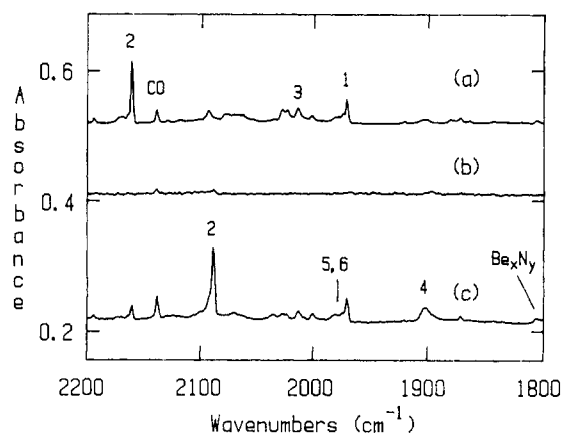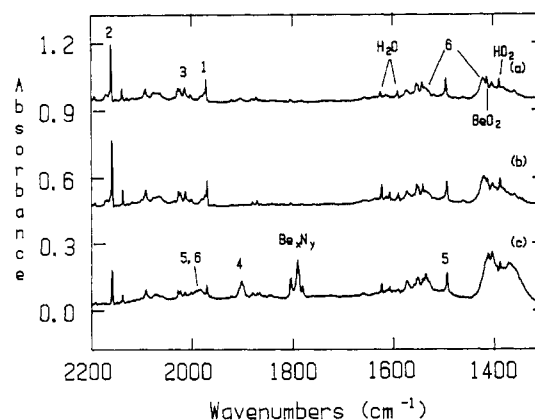

Figure 1. Infrared spectra of the 2200–1800-cm^{-1} region for samples prepared by codeposition of beryllium atoms for 3 h at 10 K with 25:1 mixtures of argon and (a) H$_2$, (b) D$_2$, and (c) HD.

Figure 2. Infrared spectra in the 2200–1800-cm^{-1} region for beryllium atoms codeposited at 10 K with a 25:1 argon/H$_2$ sample after (a) 3 h of codeposition at 10 K, (b) 30-m broad-band photolysis, and (c) matrix annealing to 30 K.

Figure 2 and can be summarized as follows. Upon annealing to 20 K, all new product bands found in this investigation grow by 5% on annealing to 20 K, due to liberation and reaction of trapped H atoms. Bands at 2159.1 and 1970.0 cm^{-1} grow by 20% on photolysis and decrease by 60% on annealing to 30 K. The band at 2013.7 cm^{-1} exhibits no change on photolysis and decreases

Reactions of Beryllium Atoms with Hydrogen

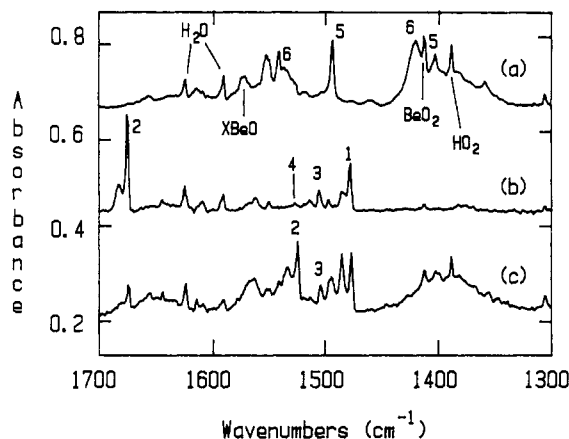*J. Am. Chem. Soc., Vol. 115, No. 25, 1993* 12113

Figure 3. Infrared spectra of the 1700–1300-cm^{-1} region for 3 h of codeposition at 10 K of beryllium atoms with 25:1 mixtures of argon and (a) H_2, (b) D_2, and (c) HD.

Figure 4. Infrared spectra in the 900–400-cm^{-1} region for 3 h of codeposition at 10 K of beryllium atoms with 25:1 mixtures of argon and (a) H_2, (b) D_2, and (c) HD.

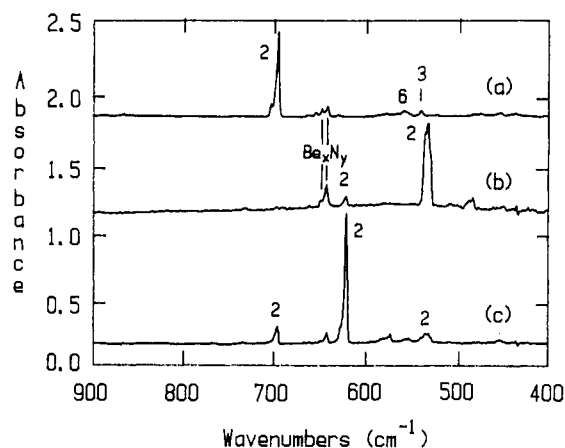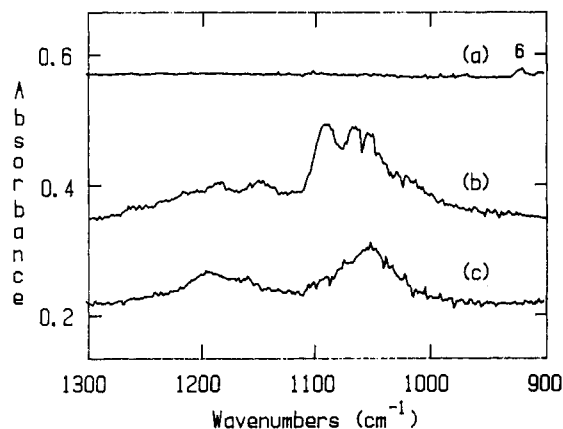**Figure 5.** Infrared spectra in the 1300–900-cm^{-1} region for 3 h of codeposition at 10 K of beryllium atoms with 25:1 mixtures of argon and (a) H_2, (b) D_2, and (c) HD after annealing to 30 K.

by 50% on annealing. The band at 1982 cm^{-1} also does not change on photolysis but grows by 50% on annealing. The 1900.6-cm^{-1} band is destroyed on photolysis but increases substantially on annealing. Finally, CO_2 and CO impurity bands are found at 2339.1 and 2138.1 cm^{-1}, respectively, and a Be_xN_y band group is centered at 1790 cm^{-1}.[27]

In the 1700–1300-cm^{-1} region, the top spectrum in Figure 3, product bands are present at 1536, 1493.4, 1420, and 1402.1 cm^{-1} (labeled 6, 5, 6, and 5, respectively). Impurity bands are found at 1623.4–1590.3 (water), 1572.5 XBeO, 1412.6 (BeO_2), 1387.5 (HO_2), and 1305.1 cm^{-1} (methane).[28,31] All product bands in this region exhibit very little change in intensity after broad-band photolysis and grow 50% upon annealing to 30 K. A strong broad band appears at 1370 cm^{-1} only after final annealing.

The top spectrum in Figure 4 shows absorption bands in the 900–400-cm^{-1} region. A strong band at 697.9 cm^{-1} (labeled 2) is immediately evident as well as a weaker absorption band at 558 cm^{-1} (labeled 6). A weak new band was observed at 540.0 cm^{-1} (labeled 3). Bands at 648.2 and 642.6 cm^{-1} have been identified as a Be_xN_y species, formed by the reaction of Be with N_2 impurity in the system.[27] Weak bands at 1130.6 and 866.0 cm^{-1} are due to (BeO)$_2$ formed by the reaction of Be atoms with trace O_2 impurity.[28]

Be + D_2. For the isotopic experiments, the term shifted is only used when the "shifted" band exhibits similar behavior on photolysis and annealing and has the same band shape. Band positions for Be_xD_y products are also listed in Table I. The 1700–1300-cm^{-1} region is shown in the middle spectrum of Figure 3 for codeposition of Be atoms with a 25:1 mixture of Ar/D_2 after 3 h. The product band at 2159.1 cm^{-1} is shifted to 1677.0 cm^{-1}. The 2013.7-cm^{-1} band is shifted to 1504.2 cm^{-1} and the 1982-cm^{-1} band is found at 1568 cm^{-1}. The band at 1900.6 cm^{-1} growing strongly on annealing is shifted to 1533.0 cm^{-1}, and lastly the 1970.0-cm^{-1} band is shifted to 1477.6 cm^{-1}. The weak band at 2088 cm^{-1} in Figure 1b is due to the HD counterpart of species 2 described below.

In the 1300–900-cm^{-1} region, shown in the middle spectrum of Figure 5, the two product band groups found between 1536 and 1402.1 cm^{-1} in the hydrogen experiments now appear as two broad bands at 1094 and 1067 cm^{-1}. The H_2 product band at 1370 cm^{-1} is shifted to 1053 cm^{-1}.

In the 900–400-cm^{-1} region, Figure 4b, it is evident that the D_2 counterpart of the 697.9-cm^{-1} band is shifted to 531.9 cm^{-1} and the 558-cm^{-1} band is shifted below 400 cm^{-1}. The band at 622.2 cm^{-1} is probably the HD counterpart of species 2. The weak band at 872 cm^{-1} is present as a weak diffuse band centered

(31) Smith, D. W.; Andrews, L. *J. Chem. Phys.* **1974**, 60, 1981. Milligan, D. E.; Jacox, M. E. *J. Chem. Phys.* **1963**, *38*, 2627.

at 651 cm^{-1} that is only discernable in experiments completely free of the Be_xN_y impurity at 642.6 cm^{-1} after annealing.

Be + HD. In the 2200–1800-cm^{-1} region, shown in the bottom spectrum of Figure 1, a new band is observed at 2088.3 cm^{-1}, which behaves the same as the 2159.1-cm^{-1} band in the hydrogen experiments. Additionally, the 1900.6-cm^{-1} band with H_2 is shifted to 1902.2 cm^{-1} with HD and both 1902.2- and 1536.8-cm^{-1} bands increase 10-fold on annealing.

In the 1700–1300-cm^{-1} region, shown in Figure 3c, a strong band centered at about 1388 cm^{-1} also grows 5-fold on annealing. There is a complicated series of bands present between 1477.6 and 1568 cm^{-1}. Of these only bands at 1524.9, 1504.9, and 1486.2 cm^{-1} are new. The bands at 1504.9 and 1486.2 cm^{-1} behave identically to the bands at 1493.4 and 1402.1 cm^{-1} present in the hydrogen experiments. The band at 1524.9 cm^{-1} increases by 30% on photolysis and decreases by 60% on annealing. The band found at 1533 cm^{-1} in the deuterium experiments increases 10-fold on annealing to 30 K and is shifted to 1536.8 cm^{-1} in the HD experiments.

In the 1300–900-cm^{-1} region, shown in Figure 5c, the band at 916.7 cm^{-1} is evident in HD experiments with good yields. However, at 1189 and 1051 cm^{-1} very broad bands without definition grow in on annealing.

In the 900–400-cm^{-1} region, shown in Figure 4c, all bands present in the hydrogen and deuterium experiments are present in the HD experiments. Additionally, a strong new absorption is now found at 622.0 cm^{-1}. This band behaves exactly the same as the 697.9- (hydrogen experiment) and 531.9-cm^{-1} (deuterium experiment) bands on photolysis and annealing, which are also
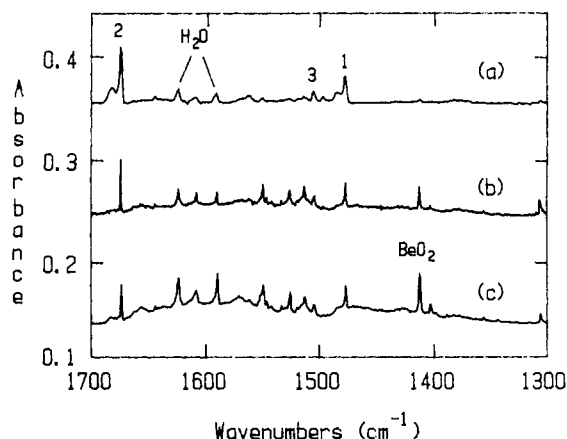
Figure 6. Infrared spectra in the 1700–1300-cm^{-1} region for 3 h of codeposition at 10 K of beryllium atoms with (a) 25:1, (b) 50:1, and (c) 100:1 Ar/D$_2$ mixtures.

observed as weak bands in the HD experiments. Annealing produced substantial growth in bands at 462.9, 463.6, and 454.8 cm^{-1}.

Concentration dependence experiments for Be + H$_2$, D$_2$, and HD were conducted to determine which products might be favored at various dilutions of hydrogen in argon. In more dilute experiments, broad bands are much lower in intensity as well as sharper in appearance, as shown in Figure 6 for the D$_2$ experiments. Overall, product bands are reduced significantly in the 100:1 experiments. Additionally, in more dilute experiments, impurity reaction products become more significant owing to the lack of reactivity of hydrogen in general.

Discussion

Evidence will be presented for the assignment of new infrared absorption bands produced by the reaction of hyperthermal beryllium atoms with hydrogen to form six product molecules: BeH, BeH$_2$, BeBeH, HBeBeH, HBeHBeH, and HBe(H)$_2$BeH. These assignments are based on photolysis and annealing behavior, isotopic shifts, and ab initio calculations at the MBPT(2) level.

BeH. The band at 1970.0 cm^{-1} in the Be + H$_2$ experiments (labeled 1) is assigned to BeH. The gas-phase value for this fundamental band is 1988.2 cm^{-1}, which yields a small common red argon matrix shift (18.2 cm^{-1}).[4,12] The calculated value for this vibrational frequency is 2086.3 cm^{-1}, which yields a 0.944 experiment/theory ratio or scale factor. The calculated BeD vibration is 1548.2 cm^{-1} where the experimental value is 1477.6 cm^{-1} (0.954 scale factor). This yields an H/D ratio of 1.3332 compared to the calculated harmonic value of 1.3476, thus demonstrating the degree of anharmonicity usually found with hydrogen vibrations. Both 1477.6- and 1970.0-cm^{-1} bands are present and unshifted in the Be + HD experiments as expected for a species containing a single H atom.

The direct mechanism for this reaction, shown in eq 1, is endothermic by 56 ± 2 kcal/mol, based on bond dissociation energies[4] and 46 kcal/mol based on the present MBPT(2) calculations.

$$Be + H_2 \rightarrow BeH + H \qquad (1)$$
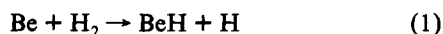
The energy required to overcome this barrier to reaction can be provided initially by the excess kinetic energy possessed by the nascent Be atoms directly after laser ablation. The 20% increase of BeH on photolysis is probably due to a combination of three mechanisms. First, since Be does absorb radiation in the UV,[32] electronic excitation of Be can input more than enough energy to overcome this barrier. Second, HBeBeH decreases significantly

Table III. Frequency Ratios (Experiment/Theory) or Scale Factors Calculated for Beryllium Hydrides[a]

molecule	terminal Be–H	H–Be–H bend	bridged Be–H–Be
BeH	0.944		
BeH$_2$	0.969	0.934	
BeBeH	0.952		
HBeBeH	0.903		
HBeHBeH	0.913		0.98, 0.93
HBe(H)$_2$BeH	0.918	0.944	0.95, 0.96

[a] Calculated from data in Tables I and II.

on photolysis, yielding two BeH molecules as likely products. Lastly, photoexcited beryllium atoms can react with free H atoms in the matrix to form BeH. The decrease of BeH observed after annealing is undoubtedly due to dimerization to form larger molecules.

BeH$_2$. Bands at 2159.1 and 697.9 cm^{-1} (labeled 2) are assigned to linear BeH$_2$. There are to date no experimental data for this molecule, but several theoretical calculations have been conducted.[3,15,16] Geometry optimization for this molecule at the MBPT(2) level yields a linear structure ($r = 1.333$ Å) with frequencies of 2228.6 (v_3), 747.3 (v_2), and 2025.2 cm^{-1} (IR inactive v_1 mode). The experiment/theory ratios are 0.969 for v_3 and 0.934 for v_2 of BeH$_2$. Complete deuterium substitution gives strong bands at 1674.0 and 531.9 cm^{-1} and experiment/theory ratios of 0.977 for v_3 and 0.925 for v_2 of BeD$_2$, which are appropriate for this level of theory.[33] Scale factors are compared in Table III for the beryllium hydrides observed in this investigation.

Two points are of interest concerning the experiment/theory ratios or "scale factors". First, note that the scale factors are similar but not identical for the v_3 (antisymmetric stretching) and v_2 (bending) modes of BeH$_2$. These modes have different anharmonicities and theory does not predict them equally well. A similar variation in scale factors has been found among the vibrational modes of B(OH)$_3$.[34] Second, the slightly different scale factors for v_3 of BeH$_2$ and BeD$_2$ and for v_2 of BeH$_2$ and BeD$_2$ attest to the difference in anharmonicities for different isotopes and vibrational modes.

The H/D ratios for v_2 and v_3 of BeH$_2$ show different anharmonicities for the bending and antisymmetric stretching modes of this linear molecule. For a harmonic oscillator, both modes should exhibit an H/D ratio of 1.3001, but the observed ratio for v_2 is higher (1.3121) and the observed ratio for v_3 is lower (1.2898). The slightly smaller observed ratio for the antisymmetric stretching mode is expected for cubic contributions to anharmonicity as described above for BeH. However, the slightly higher ratio indicates quartic anharmonicity of opposite sign in the bending potential for the linear molecule. A similar relationship exists for the v_2 and v_3 fundamentals of linear MgH$_2$ and MgD$_2$.[35]

In the Be + HD experiments, the v_1 mode for BeHD is IR active and found at 1524.9 cm^{-1} compared with the calculated value of 1551.0 cm^{-1} (0.983 ratio). Additionally, the HD counterparts of v_3 and v_2 are found at 2088.3 and 622.0 cm^{-1}. The calculations yield 2150.4 and 666.7 cm^{-1} and observed/calculated ratios of 0.953 and 0.933, respectively. In the BeHD molecule, the two stretching modes interact, share intensity, and are subsequently separated from the average of the calculated v_3 and v_1 frequencies for BeH$_2$ and BeD$_2$. Calculations predict a 4.4:1 intensity ratio for v_3 and v_1 of BeHD, which agrees well with the observed absorbance ratio of 3.5:1. Unshifted bands for BeH$_2$ and BeD$_2$ are also present in the HD experiments. This means

(32) Brom, J. M., Jr.; Hewett, W. D., Jr.; Weltner, W., Jr. *J. Chem. Phys.* **1975**, *62*, 3122.

(33) Hehre, W. J.; Radom, L.; Schleyer, P. v. R.; Pople, J. A. *Ab Initio MO Theory*, Wiley: New York, 1986.

(34) Andrews, L.; Burkholder, T. R. *J. Chem. Phys.* **1992**, *97*, 7203.

(35) McCaffery, J. G.; Parnis, J. M.; Ozin, G. M.; Breckenridge, W. H. *J. Phys. Chem.* **1985**, *89*, 4945.

that BeH_2 can also be formed via the sequential reaction,

$$H + BeH \rightarrow HBeH \qquad (2)$$

which is exothermic by 86 kcal/mol. It is of interest to note that the v_2 band position for the BeHD product does not lie exactly between the BeH_2 and BeD_2 counterparts. This is expected since the reduced mass of the light central atom beryllium makes a substantial contribution to the mass relationships.

The BeH_2 bands increase by 20% on photolysis and decrease by 60% after annealing to 30 K. The reaction of Be with H_2, shown in eq 3, is exothermic by 40 kcal/mol, based on

$$Be + H_2 \rightarrow BeH_2 \qquad (3)$$

MBPT(2) calculations, but this reaction must require some activation energy. Once formed BeH_2 is relaxed and trapped by the matrix. For the same reasons described above any barrier to this reaction can be initially overcome by the hyperthermal Be atoms from laser ablation and by electronic excitation of Be on sample photolysis. Photoexcitation of Mg atoms in the presence of H_2 has been shown to form the linear MgH_2 molecule.[35] As with BeH, annealing must yield dimerization of BeH_2 and formation of higher order molecules accounting for the significant reduction in band intensities after annealing.

BeBeH. Bands at 2013.7 and 540.0 cm^{-1} (labeled 3) are attributed to Be_2H on the basis of photolysis and annealing behavior, isotopic shifts, and theoretical calculations. MBPT(2) calculations yield a linear configuration with stretching frequencies at 2114.9 (0.952 observed/calculated ratio) and 541.7 (0.997 observed/calculated ratio) and structure given in Figure 7. In the Be + D_2 experiments, the 2013.7-cm^{-1} band is shifted to 1504.2 cm^{-1}. The calculated value for BeBeD is 1574.6 (0.955 ratio). Unfortunately, the deuterium counterpart for the 540.0-cm^{-1} band was not observed. The H/D shift ratio of 1.339 indicates a predominantly H–Be stretching motion and the observation of both BeBeH and BeBeD in the Be + HD experiments confirms the presence of a single H atom and the identification of BeBeH.

Here the bonding effect of H on the Be_2 submolecule of BeBeH is clearly illustrated. The Be–Be stretching fundamental is increased from 224 cm^{-1} for Be_2[18] to 540 cm^{-1} for BeBeH, indicating a significant strengthening of the Be–Be bond.

The Be_2 reaction, shown in eq 4, is endothermic by 16 kcal/mol, based on MBPT(2) calculations. However, the reaction of

$$Be_2 + H_2 \rightarrow BeBeH + H \qquad (4)$$
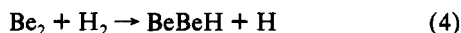
Be and BeH, shown as reaction 5, is exothermic by 30 kcal/mol

$$Be + BeH \rightarrow BeBeH \qquad (5)$$

and provides a more likely mechanism for the formation of BeBeH. Metal dimers are known to have much weaker absorptions than corresponding metal atoms in the visible and UV which may explain why BeBeH does not grow on broadband photolysis. This molecule is dipolar where the terminal beryllium atom and the hydrogen are partially negative.[16] This would facilitate hydrogen addition to yield the more stable HBeBeH product, which explains the 50% reduction on annealing for Be_2H.

HBeBeH. The band at 1900.6 cm^{-1} in the Be + H_2 experiments (labeled 4) is assigned to the linear HBeBeH dimer. MBPT(2) calculations for $(BeH)_2$ dimers reveal that the linear dimer is 44.6 kcal/mol lower in energy than the D_{2h} dimer and 56.3 kcal/mol lower in energy than HBeHBe. The theoretical prediction for the strong antisymmetric Be–H stretching mode is 2104.2 cm^{-1}; the experiment/theory ratio is 0.903. In the Be + D_2 experiments, this band is shifted to 1533.0 cm^{-1}, yielding an H/D ratio of 1.240 and indicating considerable anharmonicity, which is not surprising for a linear molecule with charge asymmetry.[16] In the Be + HD experiments, two IR active bands are found at
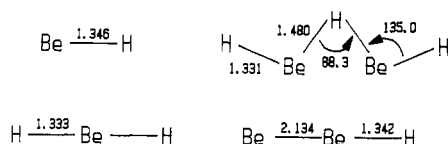

Figure 7. Stick figures and optimized geometries for BeH, BeH_2, Be_2H, and the dimerization product HBeHBeH. Distances in Å, angles in deg.

1902.2 and 1536.8 cm^{-1}. These bands differ slightly from the Be_2H_2 and Be_2D_2 counterparts, as expected for the HBeBeD molecule with little coupling between the terminal Be–H and Be–D vibrations. This is confirmed by the calculated positions of the isotopic bands (Table II).

There are at least three mechanisms whereby HBeBeH may be formed, shown in eqs 6–8.

$$2BeH \rightarrow HBeBeH \qquad (6)$$

$$BeBeH + H \rightarrow HBeBeH \qquad (7)$$
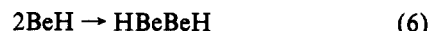
$$Be + BeH_2 \rightarrow HBeBeH \qquad (8)$$

Reaction 6 is exothermic by 69 kcal/mol, reaction 7 is exothermic by 85 kcal/mol, and reaction 8 is exothermic by 29 kcal/mol. On sample codeposition HBeBeH is probably formed whenever 2 HBe molecules are in close proximity. Since reaction products are initially trapped in an argon matrix, the yield of HBeBeH formation is small in the deposited sample. On final annealing the 1900.2-cm^{-1} band increases to ten times its initial intensity.

Broad-band photolysis causes the 1900.2-cm^{-1} HBeBeH band to disappear completely. This molecule is probably excited to a repulsive potential energy surface which can yield 2 energetic BeH molecules since diffusion and subsequent cage escape is not restricted for such small molecules in an argon matrix.[36] The Be–Be bond in the Be_2 dimer is known to be very weak, mainly a van der Waals interaction, but in the HBeBeH molecule the Be–Be bond is much stronger. In fact the Be–Be bond distance is calculated to be 0.40 Å shorter and the frequency higher (625 cm^{-1}) for HBeBeH than for Be_2. Another possible pathway for the large decrease in HBeBeH on photolysis is photodissociation to form Be_2 and H_2. This reaction is endothermic by 67 kcal/mol, but it could be accessed by broad-band photolysis.

HBeHBeH. Bands at 1493.4 and 1402.1 cm^{-1} (labeled 5) are assigned to HBeHBeH on the basis of band shape, photolysis and annealing behavior, isotopic shifts, and theoretical calculations. The optimized geometry for this molecule is shown in Figure 7. The structural parameters for HBeHBeH are close to those of $HBe(H)_2BeH$, and the vibrational frequencies are similar to those observed for $HBe(H)_2BeH$. Theoretical calculations predict five modes for HBeHBeH that should show significant IR activity; 2158.3 (B_2), 1524.0 (A_1), 1504.8 (B_2), 502.8 (A_1), and 375.2 (B_2) cm^{-1}. The mode for the band at 2158.3 cm^{-1} is very similar to that for $HBe(H)_2BeH$ predicted at 2157.9 cm^{-1}, where both bands are probably present in the broad absorption at 1982 cm^{-1}. The experiment/theory ratios for the 1493.4- and 1402.1-cm^{-1} bands are 0.980 and 0.932, respectively. While the assignment of these two bands to HBeHBeH is complicated by the close proximity of absorptions due to $HBe(H)_2BeH$, these bands are sharp while all bands attributed to $HBe(H)_2BeH$ are broad in nature. In the Be + D_2 experiments, the 1493.4- and 1402.1-cm^{-1} bands correlate with 1095- and 1053-cm^{-1} bands, respectively, of the D_2 experiments (1.331 H/D ratio).

The only plausible mechanism for formation of this molecule is dimerization of BeH with BeH_2, shown in eq 9.

$$BeH + BeH_2 \rightarrow HBeHBeH \qquad (9)$$

Reaction 9 is exothermic by 26 kcal/mol and the observed 50% growth on annealing is expected for such a ready association.

(36) Andrews, L.; Johnson, G. L. *J. Phys. Chem.* **1984**, *88*, 425.

HBe(H)$_2$BeH. Broad bands at 1982, 1536, 1420, 872, and 558 cm^{-1} (labeled 6) are assigned to HBe(H)$_2$BeH. These bands show no change during photolysis and grow by 50% on annealing. The appearance of broad bands in the 1600–1300-cm^{-1} region is indicative of bridging hydrogen atoms predicted theoretically for HBe(H)$_2$BeH[3,9,15] and well-known in the B$_2$H$_6$ molecule, H$_2$B(H)$_2$-BH$_2$ in the bridging notation. The calculated band positions are 2157.9 (0.918 experiment/theory ratio, terminal Be–H), 1600.2 (0.960, bridging Be–H–Be), 1494.7 (0.950, bridging Be–H–Be), 948.0 (0.920), and 591.2 (0.944) cm^{-1}, respectively. In the Be + D$_2$ experiments, the 1982 band is shifted to 1568 cm^{-1} (1.264 H/D ratio). The 1420-cm^{-1} band is shifted to 1067 cm^{-1} (1.33 ratio). The 872-cm^{-1} band is observed as a weak broad band at 651 cm^{-1} (1.33 ratio). The HD experiments are not as helpful in this case due to the many possible isotopic combinations (eight) that can be formed, which is evident by the strong broad bands centered at 1389 and 1050 cm^{-1}. There are several bands in the 1545–1486- and 473–435-cm^{-1} regions that exhibit appropriate photolysis and annealing behavior for this molecule, but assignments to specific H/D substituted molecules would be tentative.

There are two mechanisms whereby HBe(H)$_2$BeH may be formed, shown in eqs 10, and 11.

$$2BeH_2 \rightarrow HBe(H)_2BeH \qquad (10)$$

$$HBeBeH + H_2 \rightarrow HBe(H)_2BeH \qquad (11)$$
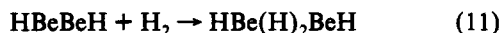
Reaction 10 is exothermic by 32 kcal/mol and reaction 11 is exothermic by 43 kcal/mol. Reaction 11 probably requires some activation energy, but reaction 10 likely does not. Therefore reaction 10 is expected to occur on annealing and to account for the 50% increase in HBe(H)$_2$BeH bands.

Finally, a strong broad band that appeared at 1370 cm^{-1} on annealing in the most concentrated experiments is characteristic of bridged beryllium–hydrogen polymeric BeH$_2$ species that are expected in the solid state. This is in excellent agreement with the broad infrared absorption near 1340 cm^{-1} for solvated solid beryllium hydride.[6]

Conclusions

Pulsed laser evaporated beryllium atoms were codeposited with argon/hydrogen gaseous mixtures onto a cold substrate. FTIR spectroscopy was utilized to identify product bands. Broad-band photolysis and annealing behavior, isotopic substitutions, and modeling by ab initio calculations were used to make band assignments. Six novel product molecules are formed from the reaction of Be atoms with H$_2$ namely BeH, BeH$_2$, Be$_2$H, HBeBeH, HBeHBeH, and HBe(H)$_2$BeH. Dimerization of the primary reaction products BeH and BeH$_2$ is found to be highly favored during annealing of the argon matrix above 20 K. The excess kinetic energy of pulsed laser ablated beryllium atoms activates reaction processes that might otherwise be inaccessible, such as the primary Be + H$_2$ reactions (1) and (3) observed here.

MBPT(2) level ab initio calculations were carried out for the H and D species to assist in these assignments as well as to provide thermochemical information. Experiment/theory ratios (scale factors) for the six beryllium hydrides characterized here are collected in Table III. Scale factors for terminal Be–H stretching vibrations range from 0.90 to 0.97 and are essentially the same for bridged Be–H–Be stretching vibrations. Note also that the terminal Be–H stretching and H–Be–H bending modes require similar but not identical scale factors.

Lastly, the matrix isolation technique employed in this work proved invaluable for providing information not obtainable in the gas phase or in bulk solids. The matrix medium provides relaxation and stabilization of the BeH$_2$ and Be$_2$H molecules that may decompose on formation in the gas phase under the energetic conditions required for reaction. Finally, dimerization of BeH$_2$ forms the hydrogen-bridged HBe(H)$_2$BeH molecule, which is a precursor to the solid-state beryllium hydride, and demonstrates how the matrix medium can isolate the gaseous molecule and subsequently allow stepwise aggregation into a solid-like species.